FRIEDRICH-ALEXANDER-UNIVERSITÄT ERLANGEN-NÜRNBERG
INSTITUT FÜR INFORMATIK (MATHEMATISCHE MASCHINEN UND DATENVERARBEITUNG)

Lehrstuhl für Informatik 10 (Systemsimulation)

Elastic Collisions in Complementarity-based Time-stepping Methods

T. Preclik and U. Rüde

Technical Report 10-9

Elastic Collisions in Complementarity-based Time-stepping Methods

T. Preclik*, U. Rüde†

2nd December 2010

Abstract. Differential complementarity problems are suited to describe a multibody system with inelastic collisions. By the example of Newton's cradle, the problems involved in treating elastic contacts are investigated. It is assessed that a proper solution requires the exact determination of impact times which stands in contrast to the time-stepping methods' idea of avoiding the collision time determination. Hence a reasonable, robust and flexible compromise is suggested which provides good results for Newton's cradle.

1 Elastic Collisions and Differential Complementarity Problems

In [12] the dynamics of rigid bodies in contact are formulated in terms of a complementarity problem, which for a frictionless contact point assumes a non-penetration constraint and the non-negativity of the contact impulses λ. Assuming the function $\Phi(\lambda, t)$ describes the contact gap, the conditions can be stated as follows:

$$\Phi(\lambda, t) \geq 0 \tag{1a}$$

$$\lambda \geq 0 \tag{1b}$$

In addition to the two constraints (1a) and (1b) the two quantities must be complementary to each other since either the bodies are in contact ($\Phi(\lambda, t) = 0$) and a contact force may act ($\lambda \geq 0$) or the bodies are separate ($\Phi(\lambda, t) > 0$) and no contact force can act ($\lambda = 0$). The complementarity is expressed componentwise with the help of the operator $\perp$:

$$\Phi(\lambda, t) \geq 0 \quad \perp \quad \lambda \geq 0 \tag{2}$$

It is important to note that this complementarity does not hold for relative contact velocities $\dot{\Phi}$. As an example consider Newton's cradle. Newton's cradle is a well-known toy often composed of 5 steel spheres suspended from strings. All of the spheres are in contact in a chain when at rest. When pulling n of the spheres to the left and letting them impact into the rest of the chain, exactly n spheres on the right side are expelled and the other spheres come to rest or remain at rest. For our purpose we consider a simplified version of the cradle, where 3 spheres each of mass m are lined up in a row. The leftmost has an initial velocity v_0 towards the other spheres at rest. Fig. 1 illustrates the configuration. We use subscripts 1 and 2 to identify the left and right contact respectively. t^- denotes the time right before and t^+ the time right after the impact occurred. Then we obtain the following values for contact impulses, contact gaps and contact velocities:

	$\lambda_1(t)$	$\lambda_2(t)$	$\Phi_1(\lambda, t)$	$\Phi_2(\lambda, t)$	$\dot{\Phi}_1(\lambda, t)$	$\dot{\Phi}_2(\lambda, t)$
t^-	0	0	0	0	$-v_0$	0
t^+	mv_0	mv_0	0	0	0	v_0

*University of Erlangen-Nürnberg, Computer Science 10, System Simulation, tobias.preclik@informatik.uni-erlangen.de
†University of Erlangen-Nürnberg, Computer Science 10, System Simulation, ulrich.ruede@informatik.uni-erlangen.de

(a) Preimpact illustration at time $t < t^-$.

(b) Postimpact illustration at time $t > t^+$.

Figure 1: Pre- and postimpact illustration of a simplified Newton's cradle.

Note that $\dot{\Phi}$ is negative for colliding contacts and positive for breaking contacts. In this case the complementarity between contact impulses and contact gaps holds, whereas the complementarity between contact impulses and contact velocities does not. This is important because rigid multibody contact problems are often formulated in terms of impulses and velocities, which seems to be wrong as also noted by the author of [2]. Furthermore the dynamics are often integrated using an implicit or semi-implicit time-stepping scheme in order to guarantee the feasibility of the constraints after each time step and to dispense with resolving collision times. Thus the complementarity between contact gaps and contact impulses then reads

$$\Phi(\lambda, t + \Delta t) \geq 0 \quad \perp \quad \lambda \geq 0. \tag{3}$$

For simplicity let us assume the time steps are of constant size Δt and that the impact occurs at a time t_0 coinciding with a time step. Then the following values result:

	$\lambda_1(t)$	$\lambda_2(t)$	$\Phi_1(0,t)$	$\Phi_2(0,t)$	$\dot{\Phi}_1(0,t)$	$\dot{\Phi}_2(0,t)$
$t_0 - \Delta t$	0	0	$v_0 \Delta t$	0	$-v_0$	0
t_0	mv_0	mv_0	0	0	$-v_0$	0
$t_0 + \Delta t$			0	$v_0 \Delta t$	0	v_0

Δt time units before the impact occurs, the leftmost sphere is $v_0 \Delta t$ away from the middle sphere and though it will approach and touch the middle sphere in the time step, it will not penetrate it. Thus no contact impulse acts and the first sphere's velocity stays at v_0. In the next time step from t_0 to $t_0 + \Delta t$, the impact occurs right at the beginning of the time step. In order to prevent penetration contact impulses mv_0 must act at both contacts. This results in new post-impact velocities, which are integrated and result in a gap forming at contact 2. This example demonstrates that the complementarity also does not hold if the post-impact relative contact velocities due to a contact reaction are non-zero since then the velocity integration leads to a non-zero gap. This non-zero gap then contradicts the complementarity condition because a contact reaction was present.

$$\lambda_2(t_0) \cdot \Phi_2(0, t_0 + \Delta t) = m \cdot v_0^2 \Delta t \neq 0 \tag{4}$$

Fig. 2 illustrates possible solutions for the impact problem above. In red the limits due to the non-negativity constraints of the contact impulses are plotted. The non-penetration constraints are plotted in green. They are calculated from the time integration of the body positions x and velocities v. Subscript indices i denote bodies or pairs of bodies for contacts forces:

$$x_i' = x_i + (v_i - \frac{\lambda_{i,i+1}}{m} + \frac{\lambda_{i-1,i}}{m}) \cdot \Delta t \tag{5a}$$

$$\Phi(\lambda, t + \Delta t) = x_{i+1}' - x_i' = \underbrace{x_{i+1} - x_i}_{\Phi(0,t)} + (\underbrace{v_{i+1} - v_i}_{\dot{\Phi}(0,t)} + 2\frac{\lambda_{i,i+1}}{m} - \frac{\lambda_{i-1,i}}{m} - \frac{\lambda_{i+1,i+2}}{m}) \cdot \Delta t \tag{5b}$$

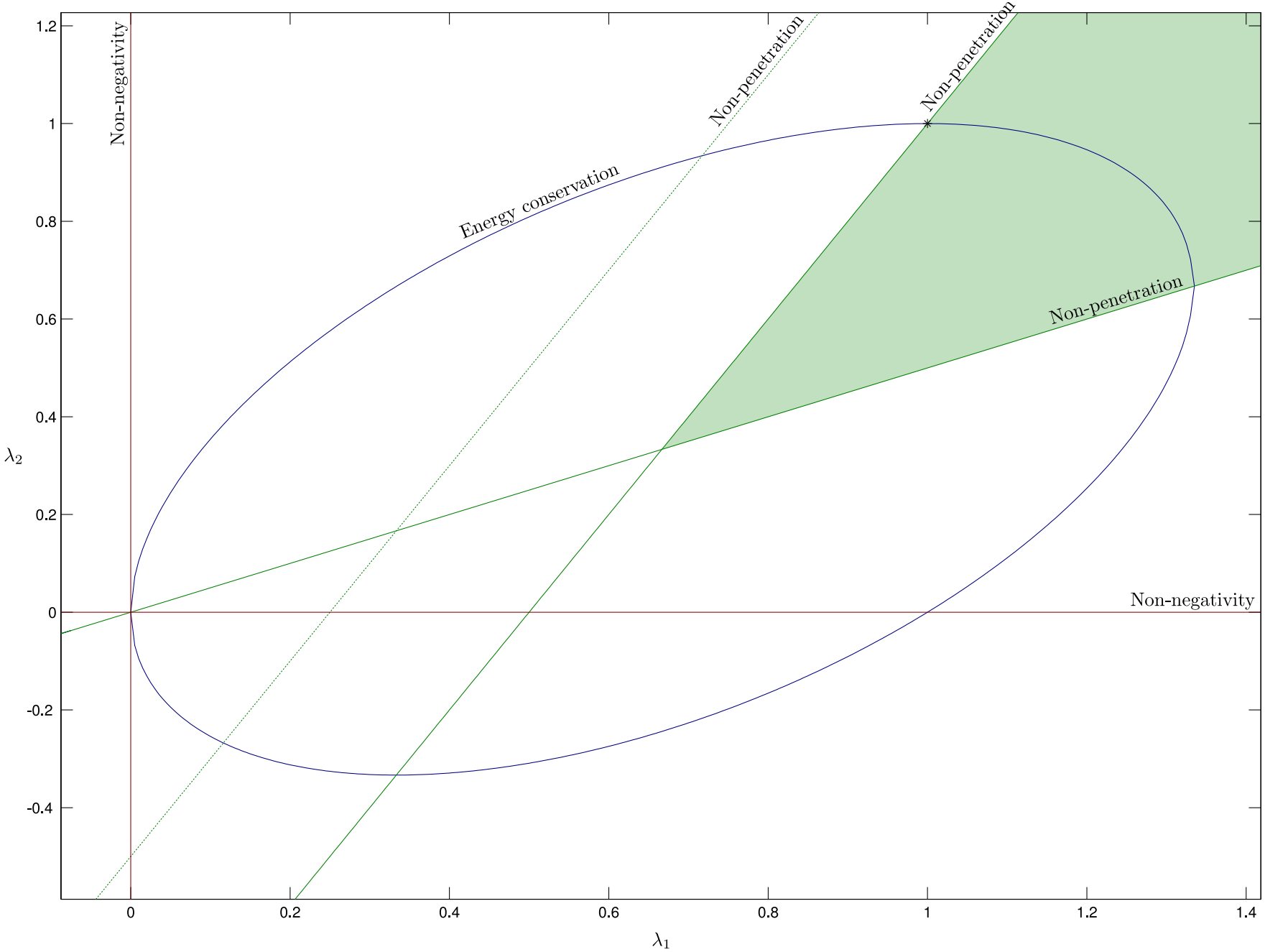

Figure 2: Solution space for the impact of one sphere into two others at rest.

$$0 - v_0 \cdot \Delta t + \frac{\Delta t}{m}(2\lambda_1 - \lambda_2) \geq 0 \tag{6a}$$

$$\lambda_2 \leq 2\lambda_1 - mv_0 \tag{6b}$$

$$0 + 0 \cdot \Delta t + \frac{\Delta t}{m}(-\lambda_1 + 2\lambda_2) \geq 0 \tag{7a}$$

$$\lambda_1 \leq 2\lambda_2 \tag{7b}$$

Thus only solutions in the upper-right cone are feasible. The expected solution as also presented in the above table is marked by an asterisk. All solutions conserving the energy are plotted in blue. These are all impulses satisfying the following equation:

$$\frac{1}{2}mv_0^2 = \frac{1}{2}m\left(\left(v_0 - \frac{\lambda_1}{m}\right)^2 + \left(\frac{\lambda_1}{m} - \frac{\lambda_2}{m}\right)^2 + \left(\frac{\lambda_2}{m}\right)^2\right) \tag{8}$$

Solving for λ_2 this leads to

$$\lambda_2 = \frac{1}{2}\lambda_1 \pm \sqrt{v_0 m\lambda_1 - \frac{3}{4}\lambda_1^2} \tag{9}$$

This shows that in contrast to common statements energy conservation, momentum conservation, non-penetration and non-negativity constraints are not sufficient to explain the behaviour of Newton's cradle. There are still an infinite number of solutions which are not the outcome of Newton's cradle. Note that all solutions are momentum conserving because the momentum added to the one object involved in a collision is subtracted from the other, thus the momentum balance is maintained.

It is also clear that all solutions require both contact impulses to be non-zero and hence the complementarity can only hold if the gaps are zero, which is only the case when both non-penetration constraints are met at the intersection of the green lines. This solution represents completely inelastic collisions, where as much energy as possible is drained from the system. The dashed green line in the figure represents the non-penetration constraint of the first (leftmost) contact if the first (leftmost) sphere has a non-zero initial gap and impacts in the middle of the first time step. However none of the solutions produces the desired outcome where the first two spheres are at rest and the third moves away with velocity v_0. If we choose λ_2 to be mv_0, then the last sphere obtains the desired momentum however since the energy conserving solution is no more on the non-penetration line, the first two spheres are separated after the time step. To be precise the first sphere remains at distance $\frac{1}{2}v_0\Delta t$ from the second sphere. When comparing this to the case where the impact occurs at the beginning of the time step but apart from this the situation is the same, then it is disturbing that the results are so different. The following table summarizes the values for the case where the impact occurs in the middle of a time step and the solution $\lambda_1 = \lambda_2 = mv_0$ is chosen:

	$\lambda_1(t)$	$\lambda_2(t)$	$\Phi_1(0,t)$	$\Phi_2(0,t)$	$\dot{\Phi}_1(0,t)$	$\dot{\Phi}_2(0,t)$
$t_0 - \frac{1}{2}\Delta t$	mv_0	mv_0	$\frac{1}{2}v_0\Delta t$	0	$-v_0$	0
$t_0 + \frac{1}{2}\Delta t$	0	0	$\frac{1}{2}v_0\Delta t$	$v_0\Delta t$	0	v_0

In summary we made the following observations when *elastic contacts* are present:

- The set of solutions varies widely.
- The complementarity conditions can only be fulfilled at the exact time of collision, does not hold for velocities at all and ceases to hold for positions shortly after impact.
- The result strongly depends on *when* within a time step the impact occurs.

This is in contrast to inelastic contacts, where there is a single correct solution[1], the complementarity conditions can be fulfilled for positions even a short time after the impact and when investigating Newton's cradle the solution, after two time steps at latest, is the same.

But how could a proper treatment of elastic contacts or non-zero restitution coefficients look like without resolving the exact time of impact? What are limitations of such an approach? And how can we characterize the desired solution?

2 On the Scent of the Right Solution

The question how we can characterize the correct solution of Newton's cradle still stands. In order to approach the answer we start by simulating the cradle with springs attached between the rigid spheres where they are in contact. As soon as the contact breaks, the springs are removed. As a first try, we employ springs acting according to Hooke's law

$$F = -kx, \tag{10}$$

where F is the restoring force, x is the displacement from the spring's equilibrium state and k is the spring constant. Fig. 3 shows a graph plotting the positions of the spheres' center of gravity over the simulation time t. In total there are 5 spheres and the upper 2 have initial velocity 1 towards the other 3 spheres. All spheres have density 1, radius 1 and no gravity acts. The compressions of the springs are plotted in the graph to the right of the positions. A negative compression indicates that the corresponding spring is inactive. In the lower-left graph the spheres' velocities are plotted. Initially the three resting spheres have velocity 0 and the two impacting spheres have velocity -1. In the lower-right graph the restoring force is plotted against the compression d. The graph shows Hooke's law for positive compressions. Unfortunately the final velocities predicted by the model do not capture the reality. The two impacting spheres slightly rebound, the remaining two inner spheres move forward with velocities around -0.5 and only one sphere is expelled on the right.

In a second attempt we model the spheres as deformable in one dimension. We discretize the sphere by cutting the sphere in n slices and replacing each slice by a mass point of appropriate mass. The mass points are connected by springs, which obey Hooke's law. The spring constant is derived by assuming a material slice between two mass points to be a flat cylinder

$$k = Er^2\pi\frac{1}{\Delta x}, \tag{11}$$

where E is Young's modulus of the sphere and r is the radius of the sphere in between the neighboring mass points. Δx is the distance between the mass points. Springs near the contacts have half the height and at their ends massless points are assumed. When in contact the two serially connected springs at the contact are replaced by a single one:

$$k_{12} = \frac{k_1 k_2}{k_1 + k_2} \tag{12}$$

The simulation results are summarized in Fig. 4. The spheres were cut into 20 slices and E was chosen to be 30. The positions graph in the upper-left now shows the position of all mass points and additionally the positions of the spheres' center of mass in thick red lines. The diagram in the upper-right again shows all spring compressions and in the lower-right the stress-strain curves are plotted for the centers of gravity. The latter

[1] To be shown in the follow-up technical report.

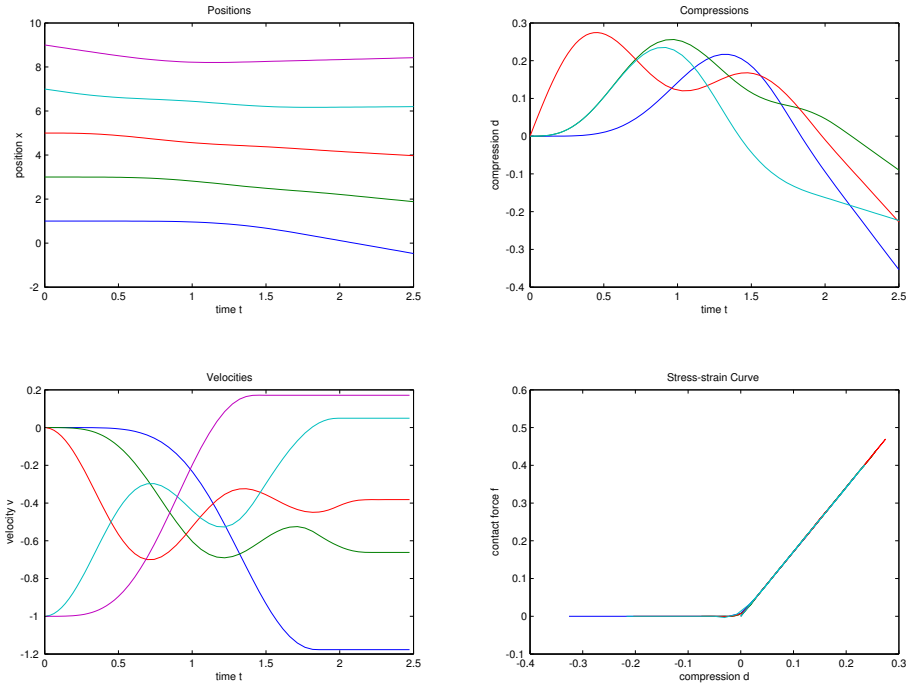

Figure 3: Simulation results for Newton's cradle with two of five spheres impacting, Hookian contact springs and rigid spheres.

are computed by differentiating the center of gravity positions twice, multiplying by the mass, which yields the force acting on the spheres' center of gravity. Then a linear least squares problem is solved to derive the effectively acting contact forces. Now the virtual contact forces are known at distinct points in time. These need to be related to the compression of the centers of gravity which are given at each time step of the ODE solver. The compression is determined by subtracting twice the radius from the distance of two neighboring centers of gravity. Negative values correspond to an extension of the virtual contact spring. A linear interpolation is used to interpolate the compressions at the points in time where the contact forces were computed. Note that all virtual contact springs approximately satisfy Hooke's law as can be seen in the lower-right diagram. The velocities are also plotted only for the centers of gravity instead of for all mass points in the lower-left diagram. In comparison to the previous model, the simulation results are in better agreement with reality though still not accurate.

Back in 1881 Heinrich Hertz published his theory about elastic bodies in contact [9]. According to his findings the restoring force is proportional to the 1.5th power of the penetration depth when two elastic spheres collide:

$$F = -kx^{\frac{3}{2}} \tag{13}$$

This Hertzian force law can be easily incorporated in our first simulation instead of the Hookian force law. Fig. 5 shows the results.

In the lower-right the Hertzian force law can be clearly identified. The sphere velocities attain values similar to those predicted by the discretized model, however they still do no reflect the ideal behaviour of Newton's cradle. The idea to further increase the exponent in the force law suggests itself and indeed as can be observed in Fig. 6, higher exponents lead to solutions resembling more the conception of an idealized Newton's cradle. Here an exponent of 5 was used. The two outer right spheres are expelled with a velocity approximately equal to the incident velocity and the remaining spheres almost come to rest.

The reason why higher exponents lead to more ideal solutions is that the force law is such that the collisions then take place one after another instead of overlapping in time. Meaning that first the second sphere collides

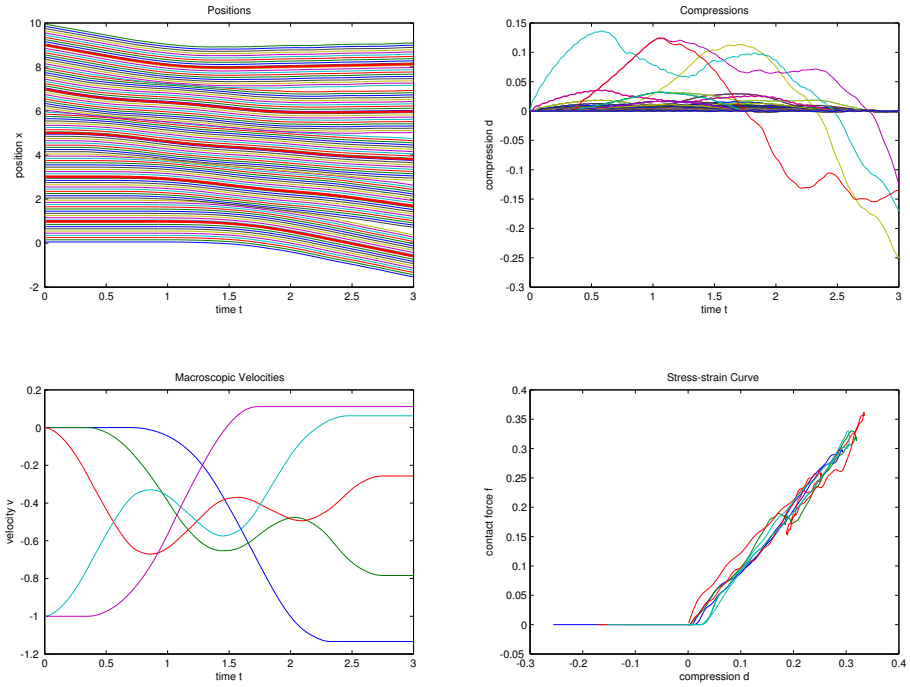

Figure 4: Simulation results for Newton's cradle with two of five spheres impacting, Hookian contact springs and Hookian material springs.

with the third, then the first sphere collides with the second sphere which just lost all of its impulse to the third and at the same time the third sphere impacts into the fourth sphere. Continuing this process leads to the ideal solution where exactly n spheres are expelled on the side opposite to the n impacting spheres. This is equivalent to a Newton's cradle where there is a gap between all spheres in the beginning.

In [8] similar simulations were performed and similar results were obtained. The authors find that a "necessary condition for the observed, simple behavior of this arrangement during collision is that the perturbation propagates throughout the system without dispersion", which is equivalent to the statement that the collisions must occur in succession. This was first published in [7] by investigating an airtrack glider experiment, where between contacting gliders a Hookian spring was placed. It was shown that when modifying the spring constants and glider masses so that the system is dispersion free, the outcome of the collision experiment matches that of an ideal Newton's cradle. However in [8] the simulations lead to the conclusion that the Hertzian force law with an exponent of 1.5 matches the reality though this setup exhibits non-negligible dispersion. The explanation the authors provide for this apparent contradiction is that after the first collision chain, the spheres are in movement and gaps form between them. Thus when the spheres swing back and the second collision sequence starts, the collisions are completely dispersion free, that is they in fact take place one after another.

3 Cylinder Collisions

In [14] the collision of cylinders is investigated thoroughly. The collision of cylinders behaves very similar to springs as also observed in [4]. When a spring impacts into a support, each ring comes to rest one after another until all rings came to rest. Then the kinetic energy is completely stored as potential energy and subsequently released. The relaxation is the time-reversed process of the compression: The outer-most twist relaxes first followed by the next inner twist until the whole spring is relaxed, which breaks the contact. This process can also be described in terms of compression waves: On impact a compressional wave is triggered at the impact point. The compressional wave travels outwards until it hits the outer end of the cylinder or spring, where it is reflected. While the compressional wave is travelling backward towards the impact point, the material relaxes

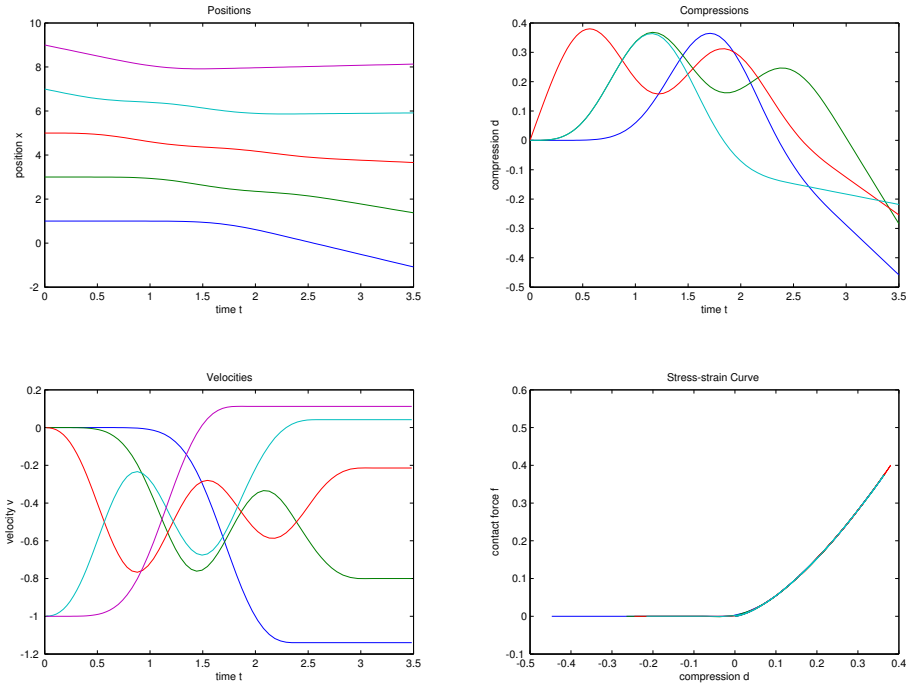

Figure 5: Simulation results for Newton's cradle with two of five spheres impacting, Hertzian contact springs and rigid spheres.

again. Thus there is a simple relationship between the length of the cylinder l, the speed of sound c and the contact time t_c — the collision lasts the time the compressional wave needs to travel to the outer end of the cylinder an back again [13]:

$$t_c = 2l/c \tag{14}$$

The speed of sound is the propagation time of the compressional wave and is readily available for cylinders of density ρ and Young's modulus E:

$$c = \sqrt{\frac{E}{\rho}} \tag{15}$$

Though the cylinder behaves like a spring when impacting, the contact force law for neither the spring nor the cylinder paradoxically behaves according to Hooke's law. Instead the contact force is constant over the time of the impact and thus independent of the compression of the spring or cylinder. This can be easily verified by modifying the simulation performed above, where we discretized the spheres in order to simulate Newton's cradle. Instead of assuming discs of different radii, the disc radii now match the cylinder radius and thus the spring constant does not vary between cylinder slices. The same holds for the mass distribution. Fig. 7 shows the results of solving the corresponding ODE with two discretized cylinders where the first one impacts into the second, resting cylinder.

Note that the stress-strain curve exhibits some overshoots resulting from the stiffness of the ODE. Furthermore the final velocity solution is not perfectly matching reality but increasing the number of discretization slices improves the result. For experimental results supporting this see [4]. Also note that the results for a cylinder-support impact are qualitatively not different.

In view of the cradle simulations above, the question arises what happens when we replace spheres by cylinders under the assumptions that the cylinders collide head-on? The simulation results are presented in Fig. 8. When comparing the velocity solution to the one presented in Fig. 6, we observe that the mechanism is completely

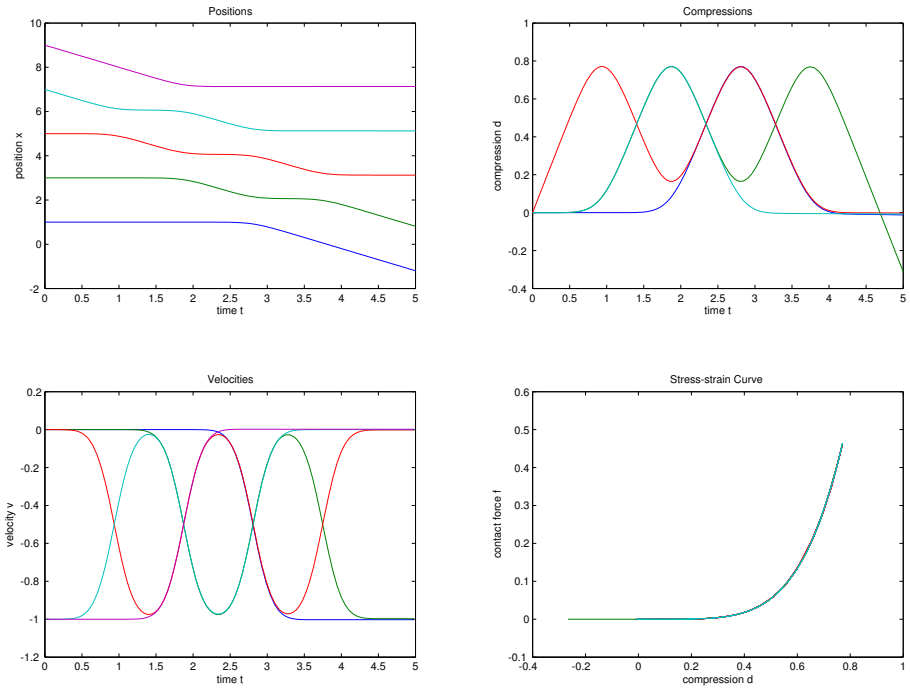

Figure 6: Simulation results for Newton's cradle with two of five spheres impacting, contact springs with a restoring force proportional to the compression raised to the 5th power and rigid spheres.

different though the final outcome is the same. Instead of being free of dispersion, the system's behavior can be explained with the help of compressional waves propagating the disturbance throughout the chain of cylinders. The time evolution of such a compressional wave is sketched in Fig. 9. The compressional wave spreads out with the speed of sound from the point of collision in both directions. The wave starts to decelerate the impacting sphere and accelerate the leftmost resting sphere. This process continues until the compressional wave hits the left end of the chain. Meanwhile the four left spheres all move with half the initial speed. The wave gets reflected on the left end and begins to stop the leftmost spheres. On the other end the compressional wave is also reflected and the rightmost spheres get their final speed v_0. This continues until the compressional waves meet again. At that point the velocities are such that contact will break.

4 Sorting out Inconsistencies

So cylinders (or springs) and spheres seem to behave fundamentally different when colliding. But what about compressional waves in sphere collisions? As discussed in-depth in [4], compressional waves also appear in sphere collisions, however the energy propagating away from the contact region is very small in contrast to the energy stored in the contact region. The latter is due to the softness of the contact region. In fact not only spheres but also short capsules (capped cylinders) and long capsules with a soft rubber tip behave the same way. The softness of the contact region is also responsible for an extended contact duration since the compression and expansion is slower. The compressional waves can in the meantime make several transits through the material whereas collisions of springs, cylinders or long capsules last for approximately a single round-trip of the compressional wave.

There is also another strong experimental evidence supporting this claim. When cylinders of unequal length collide, the compressional waves do not meet at the point of separation. Fig. 10 illustrates the wave propagation. At the point in time where the left end of the compressional wave reaches the point of origin, the right end has not yet returned but hits the end of the cylinder (assuming it is twice as long). From that moment on the compressional waves keep bouncing back and forth in the longer cylinder and the cylinder separates

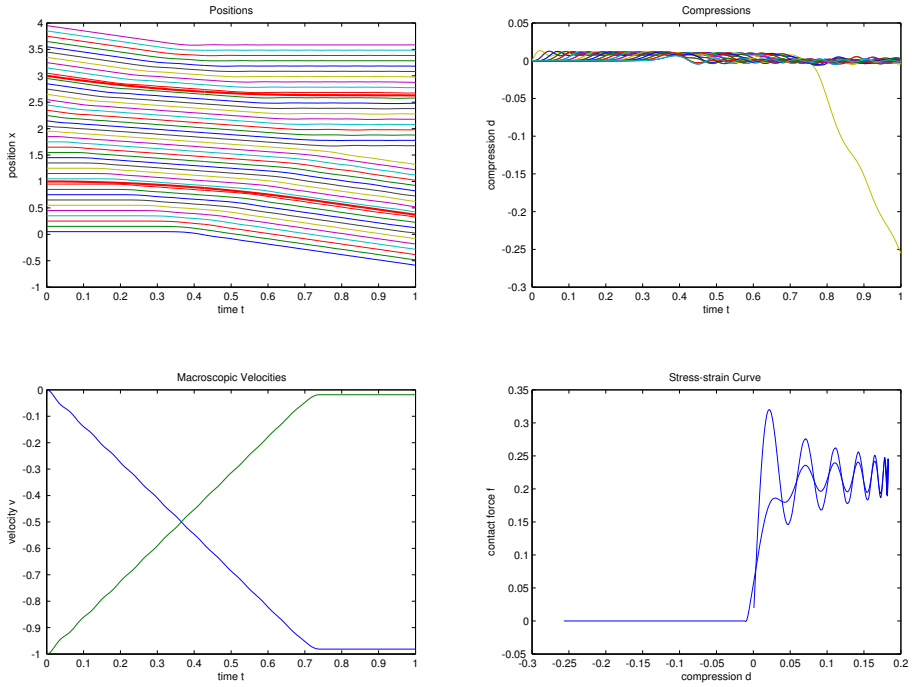

Figure 7: Simulation results for a moving cylinder impacting into a resting cylinder, a Hookian contact spring and Hookian material springs.

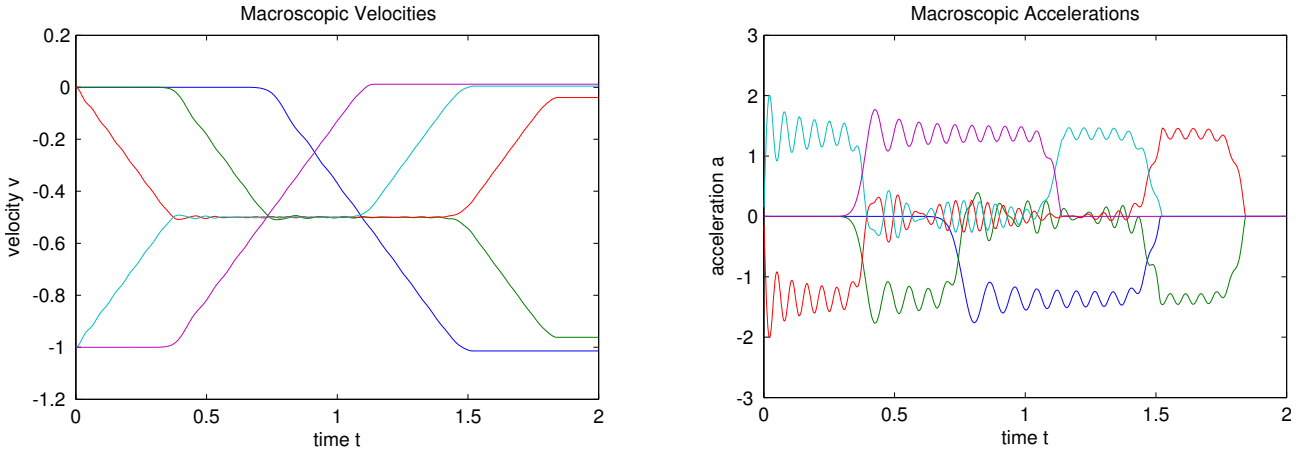

Figure 8: Simulation results for a Newton's cradle with cylinders.

from the other cylinder with an average speed of $\frac{1}{2}v_0$. The remaining (half of the initial) energy is lost as vibrational energy in the longer cylinder. Fig. 11 shows the corresponding simulation results. Note that for the longer cylinder the velocity of the center of gravity of the first and second half are plotted separately to better illustrate the oscillating behaviour. The velocity diagram matches closely the compressional wave illustration. This loss of energy as vibrational energy is not as pronounced when spheres of unequal size collide indicating that compressional waves play a minor role in sphere collisions.

5 Previous Approaches

Several approaches have been suggested before to deal with elastic contacts in complementarity-based time-stepping methods. In [5] a modification of the right-hand side was suggested depending on the velocities at the beginning of the time step. Instead of requiring a non-negative relative contact velocity to guarantee non-penetration a relative contact velocity greater equal $-k\dot{\Phi}(0,t)$ is demanded — a straight-forward implementation

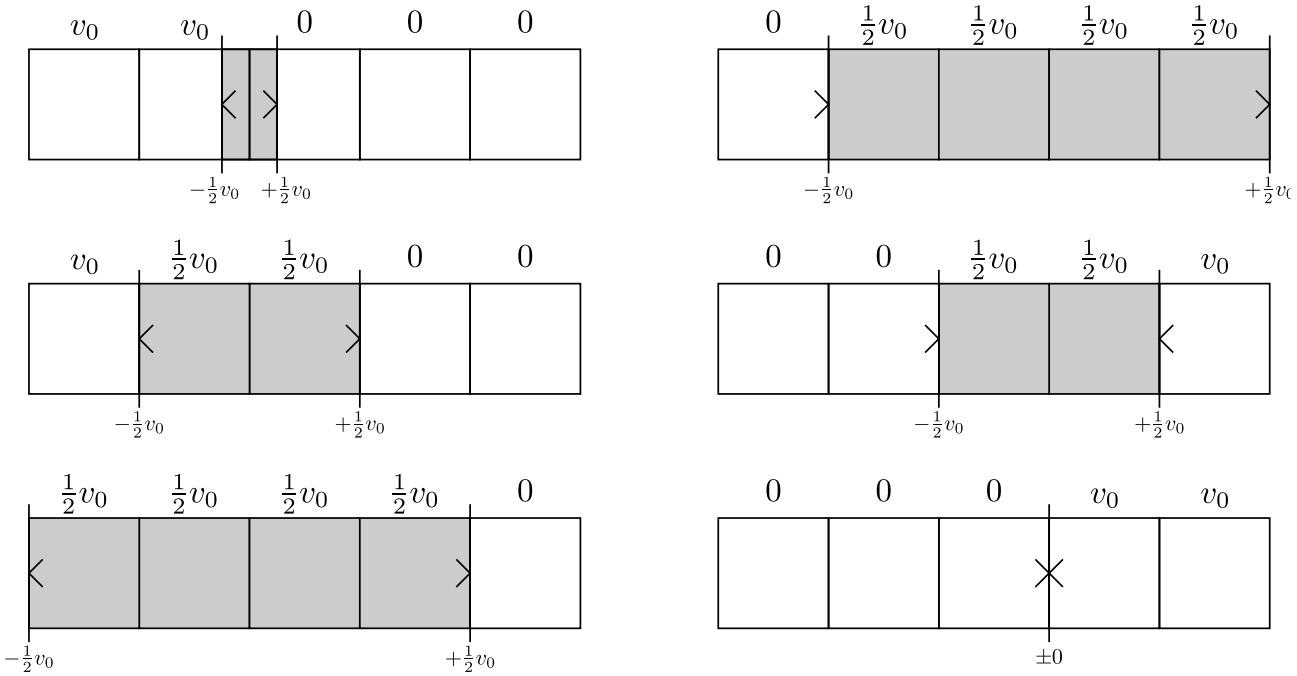

Figure 9: Cross-sectional illustration of compressional waves in a Newton's cradle with cylinders.

of Newton's hypothesis. This approach has the disadvantage that it is not clear whether the collision actually takes place or not when constructing the right-hand side. The collision actually occurs when the corresponding Lagrange multiplier λ_i is non-zero, which is decided upon only in the course of the solution process.

A different approach was tested by Anitescu and Potra in [1]. There they employed Poisson's hypothesis, which divides a collision into a compression and restitution phase. The compression phase ends when the point of maximum compression is reached and the relative normal contact velocity vanishes. The hypothesis states that the total impulse in normal direction acting at the contact is then $(1 + k)\lambda_i$, where λ_i is the impulse which acted until maximum compression was reached [11]. That this approach does not necessarily lead to the desired solution for multiple simultaneous collisions can also be seen by inspecting Newton's cradle. In the case of one sphere impacting into two resting ones, the inelastic solution is $\frac{2}{3}mv_0$ at the left contact and $\frac{1}{3}mv_0$ at the right contact. Assuming completely elastic contacts where $k = 1$, Poisson's hypothesis states that the total normal contact impulses are $\frac{4}{3}mv_0$ and $\frac{2}{3}mv_0$, which leads to the velocity solution, where the impacting sphere rebounds ($v_1 = -\frac{1}{3}v_0$) and the other two spheres move forward together ($v_2 = v_3 = \frac{2}{3}v_0$). Though the solution satisfies all constraints posed, it is not dispersion-free.

It must also be noted that hypotheses for elastic collisions like those by Newton or Poisson are only suited for two-body collisions of spheres [10]. Neither of them does for example account for vibrational energy loss. They also state nothing about simultaneous collisions of multiple bodies.

6 Time-stepping and Dispersion-free Elastic Collisions

Let us draw some conclusions. Implicit time-stepping methods try to avoid resolving the exact time of impact. Instead they try to enforce contact conditions at the end of each time step by applying an impulse at the beginning of the time step. The complementarity condition does hold for elastic contacts, when considering the exact time of impact. However the complementarity condition does not hold (neither for velocities nor for positions) for any post-collision time, since necessarily a gap forms due to the non-zero separation velocity at

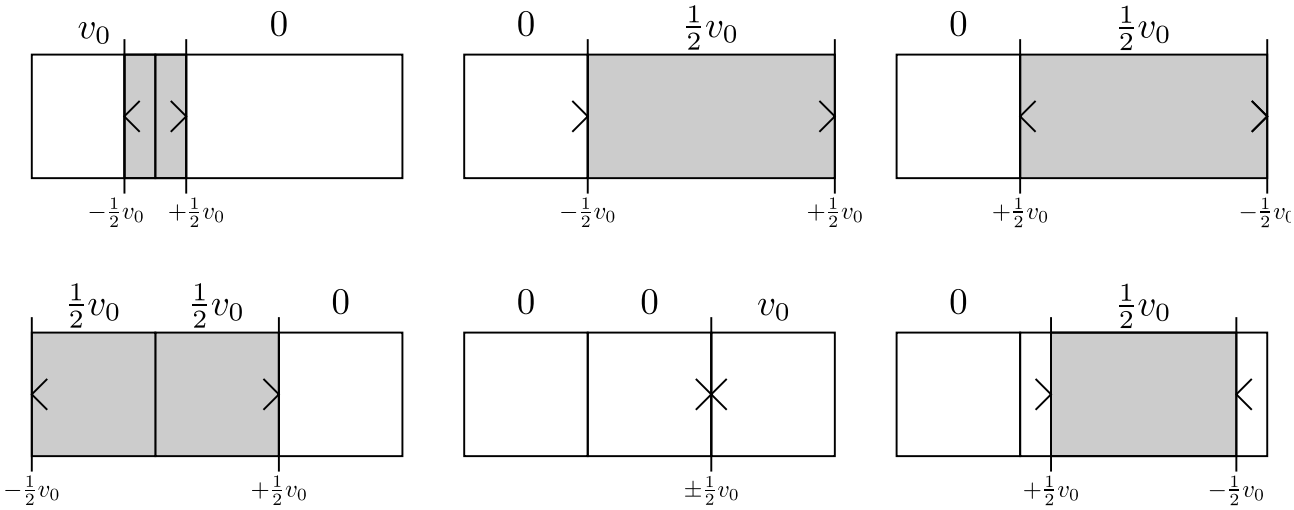

Figure 10: Cross-sectional illustration of compressional waves in two rods of unequal length.

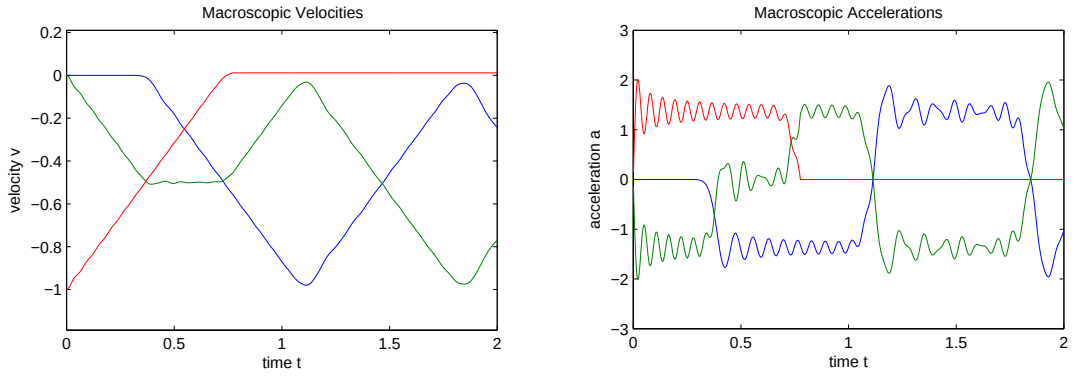

Figure 11: Simulation results for a collision of two cylinders of unequal length, Hookian contact springs and Hookian material springs.

the contact. Hence we cannot enforce them in a time-stepping scheme which avoids resolving exact impact times.

There is one obvious solution to this: Resolve collision times. At the point in time when the collision takes place, the complementarity condition holds and we can choose any solution satisfying the non-negativity, non-penetration, momentum conservation and energy conservation conditions. That is in the example of the Newton's cradle with three spheres, the solutions on the blue line between the non-penetration constraints in Fig. 2. Which one exactly is determined by the elastic properties of the involved bodies. The appropriate impulses are applied and the time-integration continues until the next impact occurs. This approach works well for elastic contacts but becomes problematic for inelastic contacts, where contacts persist and time-integration cannot move forward since actually impacts occur continuously and no progress is made in time.

For implicit time-stepping schemes it is the other way round. Inelastic contacts do not pose a problem but elastic contacts do. The question is whether we can find a compromise, which allows us to simulate elastic contacts without resolving collision times. One way to deal with it could be to assume all contacts to be inelastic. Then one can compute impulses that satisfy the complementarity constraints at the end of the time step. These impulses are applied and the bodies are time-integrated until the end of the time step. By inspecting the solution we know at which contacts impacts occurred ($\lambda_i > 0$) and where not ($\lambda_i = 0$). We also have pre-impact velocities ready at hand. From these informations we can compute a new velocity distribution which can be for

example dispersion-free and energy conserving, replacing the previously computed velocities.

In the case of a 1D chain of spheres this could be done by a simple fixed-point iteration f. In one fixed-point iteration we successively collide pairs of neighboring bodies i and $i+1$ if the velocities are directed towards each other.

$$f_{i,i+1}(\vec{v}) = \begin{cases} (v_1, \ldots, v_{i-1}, \frac{m_i v_i + m_{i+1} v_{i+1} - k m_{i+1}(v_i - v_{i+1})}{m_i + m_{i+1}}, \frac{m_i v_i + m_{i+1} v_{i+1} - k m_i (v_{i+1} - v_i)}{m_i + m_{i+1}}, v_{i+2}, \ldots, v_n)^T & \text{if } v_{i+1} < v_i \\ \vec{v} & \text{else} \end{cases} \tag{16}$$

The term in the upper branch is simply a partly elastic collision between two bodies of masses m_i and m_{i+1}, velocities v_i and v_{i+1} and a coefficient of restitution k. As initial velocities the impact velocities are taken. Since the exact impact velocities are unknown the velocities at the beginning of the time step serve as an approximation. The final fixed-point iteration is the composition of all $f_{i,i+1}$:

$$f = f_{n-1,n} \circ \cdots \circ f_{2,3} \circ f_{1,2} \tag{17}$$

For partly elastic collisions, the energy is reduced in each iteration until the iteration eventually converges. In the case of completely elastic collisions, loosely speaking the iteration transports collisions towards free boundaries. The outer spheres will then obtain separating velocities. This does not work in general for completely elastic collisions. The iteration does not converge if the collision is for example reflected at an immobile object ($m = \infty$) at both ends. Another example would be a sphere with non-zero velocity encircled by a frame (similar to billiard balls in a frame before the break). Assuming the frame and sphere are of equal mass, the objects switch their velocities infinitely while the collisions are alternating between the left and right contact.

The simulation of Newton's cradle with 5 spheres and 2 of them impacting leads to the following inelastic solution assuming no gaps exist initially:

$\lambda_{1,2}$	$\lambda_{2,3}$	$\lambda_{3,4}$	$\lambda_{4,5}$
$0.6mv_0$	$1.2mv_0$	$0.8mv_0$	$0.4mv_0$

These impulses are such that all spheres move with identical velocities after the impact ($\frac{2}{5}v_0$). The time-integration leads to a positional shift by $\frac{2}{5}v_0\Delta t$ of all spheres. Then the fixed-point iteration is evaluated and leads to the expected result that $v_1 = v_2 = v_3 = 0$ and $v_4 = v_5 = 1$. When considering cases where an initial gap exists between the impacting spheres and the others, then the final solution is not fundamentally different — only the positional shift slightly differs.

The disadvantages of this approach become clear when dealing with problems where the collision frequency is high and multiple collisions should occur within a single time step. For example when a ball is dropped on the ground and the contact is modelled as a partially elastic contact, then the collision frequency increases from bounce to bounce and soon multiple collisions per time step would take place. However the approach proposed cannot handle cases where after a collision the object moves some distance and impacts again though the time step has not ended yet. The only way to handle cases like that properly would be to resolve collision times.

7 Conclusion

In this report the problems occurring when trying to simulate elastic contacts with a complementarity-based time-stepping approach were demonstrated by means of Newton's cradle. It became clear that the complementarity condition does not hold for *elastic contacts* shortly after an impact. Instead of resolving the exact

collision times, which can be troublesome or infeasible for complex bodies, an idea was presented, how elastic contacts can still be treated. The suggested scheme allows one to easily replace the elastic collision treatment. Alternative schemes are possible where other velocity solutions can be obtained, for example by solving the wave equation, which would make it possible to account for energy lost through vibrations. Though only a one dimensional proof of concept implementation was presented, the scheme can be extended in a straight forward way to three dimensions.

References

[1] M. Anitescu and F.A. Potra. Formulating dynamic multi-rigid-body contact problems with friction as solvable linear complementarity problems. *ASME Nonlinear Dynamics*, 14:231–247, 1997.

[2] A. Chatterjee. On the Realism of Complementarity Conditions in Rigid Body Collisions. *Nonlinear Dynamics*, 20:159–168, 1999.

[3] R. Cross. The bounce of a ball. *American Journal of Physics*, 67(3):222–227, 1999.

[4] R. Cross. Differences between bouncing balls, springs, and rods. *American Journal of Physics*, 76(10):908–915, 2008.

[5] K. Erleben. Stable, Robust, and Versatile Multibody Animation. Technical report, University of Copenhagen, 2005.

[6] J.D. Gavenda and J.R. Edgington. Newton's Cradle and Scientific Explanation. *The Physics Teacher*, 35:411–417, 1997.

[7] F. Herrmann and P. Schmälzle. Simple explanation of a well-known collision experiment. *American Journal of Physics*, 49(8):761–764, 1980.

[8] F. Herrmann and M. Seitz. How does the ball-chain work? *American Journal of Physics*, 50(11):977–981, 1982.

[9] H. Hertz. Ueber die Berührung fester elastischer Körper. *Journal für die reine und angewandte Mathematik*, 92:156–171, 1881.

[10] T. Liu and M.Y. Wang. Computation of Three-Dimensional Rigid-Body Dynamics With Multiple Unilateral Contacts Using Time-Stepping and Gauss-Seidel Methods. *IEEE Transactions on Automation Science and Engineering*, 2(1):19–31, 2005.

[11] B. Mirtich and J. Canny. Impulse-based simulation of rigid bodies. In *Proceedings of the 1995 symposium on Interactive 3D graphics*, 1995.

[12] T. Preclik, K. Iglberger, and U. Rüde. Iterative Rigid Multibody Dynamics. In *Proceedings of Multibody Dynamics 2009 (ECCOMAS Thematic Conference)*, 2009.

[13] P. Roura. Collision Duration in the Elastic Regime. *The Physics Teacher*, 35(7):435–436, 1997.

[14] P. Roura. Collisions Between Rods: A Visual Analysis. *The Physics Teacher*, 41(1):32–35, 2003.

[15] D. Stoianovici and Yildirim Hurmuzlu. A Critical Study of the Applicability of Rigid Body Collision Theory. *ASME Journal of Applied Mechanics*, 63(2):307–316, 2001.